Role of Mobile Phases in the Crystallization of Polyethylene. 1. Metastability and Lateral Growth

S. Rastogi,*,† M. Hikosaka,‡ H. Kawabata,§ and A. Keller

H.H. Wills Physics Laboratory, Royal Fort, Tyndall Avenue, Bristol BS8 1TL, U.K.

Received December 12, 1990; Revised Manuscript Received June 10, 1991

ABSTRACT: As part of a more comprehensive investigation of following crystallization of polyethylene isobarically and isothermally at preselected portions of the pressure (P) and temperature (T) phase diagram within the P range of 2–5 kbar and supercoolings (ΔT) up to 10 °C, the present work is centered on formation, lateral growth (including measurement of growth rates), and melting of crystals. In the course of it the salient observation was made that, within the above specified P and ΔT range at least, all crystal growth occurs in the hexagonal phase, and only in this phase, irrespective of whether in the hexagonal (h) or orthorhombic (o) stability regime of the P–T phase diagram. In the latter case the h crystals represent a metastable form and transform into the stable o phase at some stage of growth, when, as now observed, all growth stops. The observed lower melting temperature of the h phase in the appropriate portion of the P–T phase diagram ("below" the triplet point) is consistent with all the above and introduces a newly recognized "nongrowth" region in the phase diagram. The lateral growth measurement of h crystal (the only crystals which are seen to grow) is readily interpretable by an activated growth mechanism when referred to the supercooling in the h form (as opposed to the o form, even when the latter is the stable one). Here the barrier attributable to nucleation is largely uneffected by P, but the preexponential (including transport) is retarded by increasing pressure. The implications of these findings for polymer crystallization are discussed, at this stage, in a provisional manner.

1. Introduction

As well-established, flexible polymer chains crystallize in a chain-folded manner, giving rise to lamellar crystals, where the lamellar thickness is much thinner than the fully extended chain length. By existing conceptions this does not correspond to the thermodynamically stablest form but occurs due to kinetic reasons. Namely, crystallization can take place faster through chain folding, where the chains need to deposit continuously only along a fraction of their lengths, provided, of course, that the resulting crystal is still stable at the prevailing supercooling. In contrast, the thermodynamically stablest form should correspond to crystals with extended chains, a state which normally is not realizable during primary crystal growth because of a high activation barrier to such an extended-chain deposition, whether enthalpic (large surface free energy[1]) or entropic (low-deposition probability[2]), making such crystal growth prohibitively slow.

The trend toward the above state of higher stability is nevertheless apparent by the well-established fact that chains, once deposited in a folded form, tend to extend subsequently. This may occur still during growth of the crystal at the same, isothermal, temperature of crystallization (T_c) or on subsequent heating of the crystal, normally referred to as annealing. However, such post-crystallization chain extension, normally envisaged through chain-sliding diffusion within lamellae,[3] usually only leads to rather limited crystal thickening, by about a factor of 3–4×, which, except for very short chains, is still far from full chain extension in a conventional high polymer. Here these thin lamellar crystals are denoted as F crystals.

To quote typical figures for polyethylene (PE), when PE crystallizes at atomospheric pressure, initial fold lengths, depending on supercooling, are in the range of 100–200 Å, which may extend subsequently to 300–600 Å, but to hardly more, with the sample retaining the characteristic properties of a semicrystalline thermoplastic.

A totally different form of crystallization does, however, occur at appropriately elevated pressures (thousands of bars). Here the lamellae can be several microns thick. Irrespective of whether these correspond to chains which are fully extended or whether they may still be folded a very few times (depending on the length of the chain), the resulting materials are sufficiently distinct to form a class of their own, referred to as extended (Wunderlich)[4] or extended-chain type (Bassett)[5] crystals, here to be denoted collectively as E crystals. They can be closely 100% crystalline when they are correspondingly brittle, more like a conventional polycrystalline solid. A common underlying feature of all such crystals is that they have grown in a high-entropy hexagonal (see, e.g., refs 6, 7, and 17) as opposed to the conventional orthorhombic phase (in the case of PE), where the former (for PE) is only stable at high pressure (beyond ~3.3 kbar). This highly mobile, in fact mesomorphic (Bassett,[6] Ungar[7]), hexagonal phase is only identifiable at the elevated temperature and pressure of crystallization itself: it transforms to the orthorhombic phase after cooling and removal of pressure, the conditions of usual structure examination.

There is no unanimity in regards to the exact causal relation between the hexagonal structure and spontaneous chain extension under these conditions of crystallization. By some views such chain extension arises through lamellar thickening of an initially folded structure;[8] by others it should arise directly.[9] Thinner, tapering edges, indicative of initial chain folding at the leading crystal face, were seen in situ during growth optically;[10] in the same works a close relation between the formation of the E form and a disordered mobile hexagonal phase was stressed, but from the sum total of papers it is not quite clear whether such a relation is strictly necessary or not.[8-11]

From the previous work by Bassett and co-workers,[5,6] and later followed by the other workers, P–T phase diagrams using differential thermal analysis (DTA) have been constructed such as in Figure 1. It has always been

† Permanent address: Department of Physics, Lucknow University, Lucknow 226007, India.
‡ Present address: Department of Polymer Materials and Engineering, Yamagata University, Yamagata, Yonezawa 992, Japan.
§ Present address: Nippon Petrochemical Co., Ltd., Kawasaki, Kanagawa, Japan.

0024-9297/91/2224-6384$02.50/0

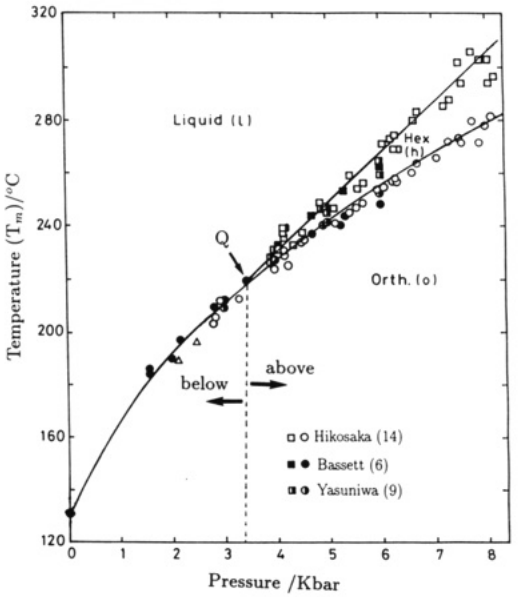

Figure 1. P–T phase diagram as observed by DTA.

thought that crystallization above the triple point Q will occur in the hexagonal (h) phase, whereas below Q it would do so in the stable orthorhombic (o) phase directly. The present work will demonstrate that, at least in the P–T domain of the phase diagram explored so far, there is no crystallization directly into the o phase, not even within the stability region of the o phase; instead, the liquid → crystal phase transformation always proceeds via the h phase even in those portions of PT space where the latter is metastable. Under these conditions equilibrium thermodynamics ceases to be of guidance and the phase diagram needs extending so as to include also the demarcation of metastable and virtual phases; this is carried out in this paper. We shall also measure lateral growth rates, for the first time under both isothermal *and* isobaric conditions, with due regard to the newly extended phase diagrams. The latter, coupled with thickness measurements (paper in preparation), will provide new and unexpected insight into the growth of these crystals with potential implications for the wider subject of polymer crystallization.

2. Experimental Section

The material of our studies was PE of $M_w = 32 \times 10^3$ with $M_w/M_n = 1.11$ (NBS fraction SRM 1483), i.e., of narrow molecular weight distribution. It was crystallized at preselected constant temperatures and pressures within a piston cylinder type high-pressure cell. The latter had transparent diamond windows through which individual crystals were observed by polarizing optical microscopy.[12] As in previous studies, they were seen to emerge and grow as isolated "cigar"-shaped uniformly birefringent objects, which have been shown by X-ray methods[13] and by optical microscopy to be single crystals (Figure 2). At appropriate stages of growth, the system was "pressure quenched" within a few seconds, when the rest of the material crystallized in a fine-grained texture leaving the initially grown larger crystals distinct.

3. Results and Discussion

3.1. Crystallization and Melting Behavior below the Triple Point. Figures 2–4 display the in situ crystallization behavior as seen optically in transmitted light between crossed polaroids at the desired temperature and pressure for the prerequisite crystallization time.

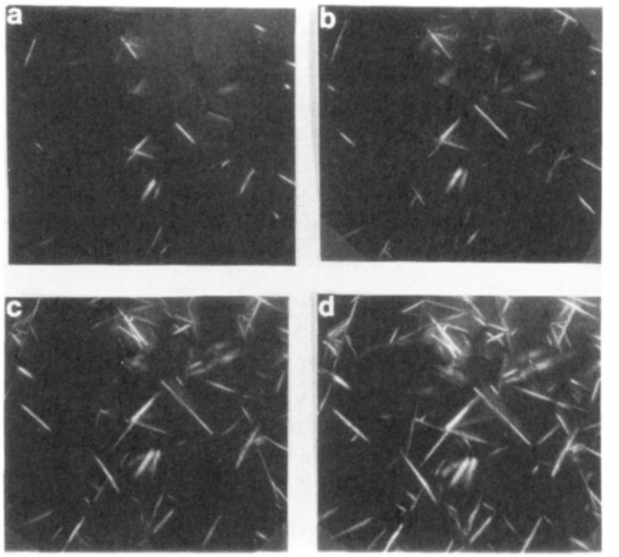

Figure 2. In situ optical micrographs during isobaric and isothermal crystallization, P = 3.94 kbar, $(\Delta T)_h$ = 3.3 °C. Different stages of crystallization at 19, 64, 119, and 139 min are shown in a–d, respectively. Scale bar = 50 μm.

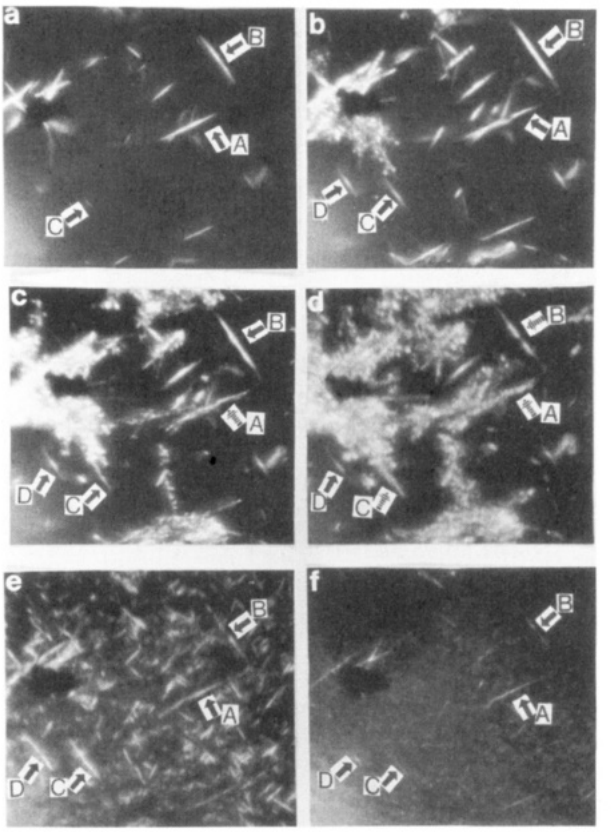

Figure 3. Growth and melting behavior above the triple point at the isobaric condition P = 4.0 kbar. a–d show in situ crystallization at different stages during isobaric conditions, P = 4.0 kbar and $(\Delta T)_h$ = 8–10 °C. e exhibits the transformed o to h crystals just before melting. f shows the melting of h crystals. Scale bar = 50 μm.

These optical micrographs show bright, line-shaped objects, against the dark background of the melt. From preceding experience these objects are lamellar crystals as viewed edge on, i.e., in the orientation where their visibility is highest. On insertion of a first-order red wave plate, in the initial stage of crystallization, crystals will appear blue or orange according to whether their long direction is perpendicular or parallel to the slow direction of the wave plate, indicating that the chain direction is

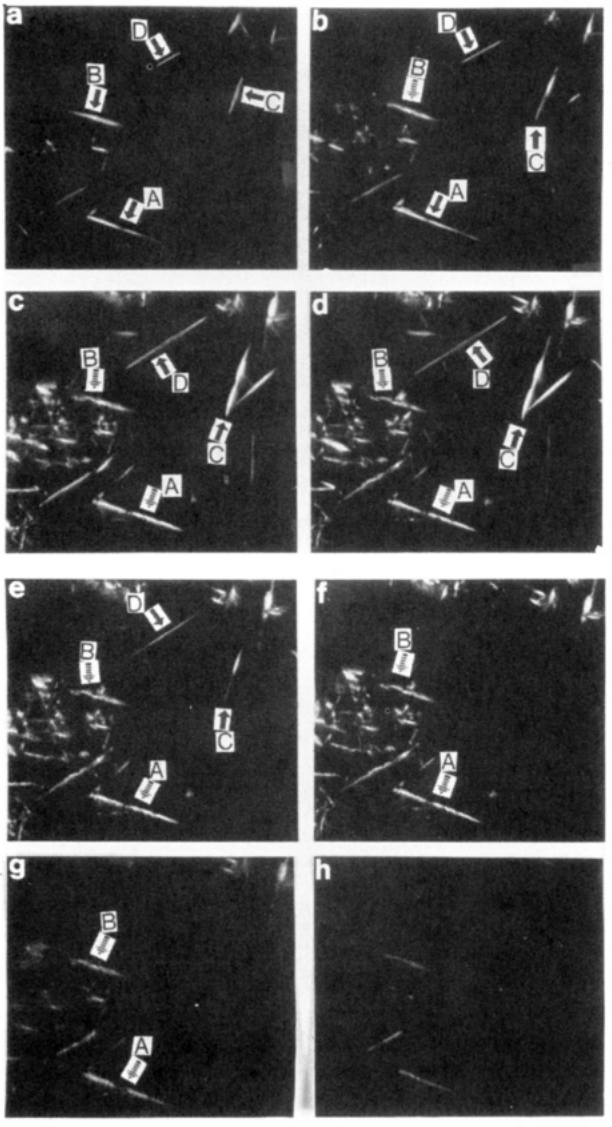

Figure 4. Growth and melting behavior of crystals below the triple point at the isobaric condition $P = 2.82$ kbar. Different stages of in situ crystallization at fixed $P = 2.82$ kbar and $(\Delta T)_o = 7$ °C for 62, 70, 95, and 101 min are shown in a–d, respectively. On raising temperature at fixed $P = 2.82$ kbar h crystals melt before the o crystals (e and f). The melting of the o crystals still at higher temperatures is shown in g and h. Scale bar = 50 μm.

normal to the crystal layer. As crystallization proceeds, the initially yellow crystals became colored and crossed by fringes following the retardation color spectrum in accordance with the above assignment of polarizabilities, hence, chain direction.

It will facilitate presentation if at this stage we introduce distinction between two kinds of crystal which will be featured throughout in what follows. In one class, as in Figure 2, the crystals are seen as uniform bright streaks with rather regular outlines. In the other class the bright streaks are seen as "blotchy" with a sequence of bright and dark patches and rather irregular outlines as, e.g., crystal A in Figures 3c,d and 4c,d. In the course of the work this distinction has emerged as basic. It is much more conspicuous on direct viewing than in the photographs and particularly so when the smooth crystals are seen to change suddenly into blotchy ones in the course of their development (see below). Separate X-ray diffraction in the course of the present program[15,16] has revealed that the smooth, uniform crystals are in the hexagonal (h) and the blotchy irregular ones in the orthorhombic (o) phase. This is an important identification enabling us to distinguish between the two crystal structures by the much more readily accessible, even if empirical, visual criterion, or, conversely, to attribute crystallographic significance to visually registered differences. (The same attribution has been made previously by Bassett, who observed equivalent changes in image on cooling;[17] we can now substantiate this by in situ X-ray diffraction[12] without relying on the phase diagram, which, as the present work will show, does not provide reliable guidance any longer. The above attribution of visual appearance to phase type, and vice versa, is an empirical fact without any obvious a priori foundation. We can say with reasonable certainty that the appearance of blotchyness is not due to overgrowth as this, by speed photography, was observed to arise within 0.04 s, which is far too fast compared to any crystal growth at the ΔT's concerned. While we cannot explain the attribution of appearance to crystal structure, we are confident in the reality of this attribution. Namely, the fact that the crystal has basically changed on the visually registered transformation is consistent with all the experimental material in this paper: as will be shown, both growth properties and melting behavior are profoundly affected, providing self-contained support to the contention that crystals start life in a phase which is metastable with a subsequent transformation to a stable phase with drastic effects on thermal stability and growth rate.)

Throughout the work we shall observe the formation of, and changes in, crystals under conditions which are simultaneously isobaric and isothermal at preselected points in the P–T phase diagram. In doing so, we shall refer to "regions" within the P–T phase diagram which, for ready reference, are marked in Figure 1. The regions are as follows: hexagonal (h) and orthorhombic (o), with the latter subdivided into regions "below" and "above" (both in terms of P) the triple point (Q).

In the course of the experiments we observed and followed the appearance and growth of crystals isobarically and isothermally in the above three regions, i.e., hexagonal and orthorhombic, in the latter case both above and below Q, and also the melting behavior in each case when heating the crystals as formed at constant P. The series in Figures 2–4 provide representative examples of our principal findings. Within a given figure consecutive frames show the same area within which given crystals can be identified, together with changes occurring in regards to their size and appearance as a function of time and in response to changes in temperature. We shall itemize these in what follows.

Figure 2 represents crystallization within the hexagonal (h) phase region. As already referred to, it reveals uniformly bright crystals appearing and growing, which by our optical criterion (based on the underlying X-ray diffraction as explained above) are in the h phase, as to be expected.

Figure 3 represents crystallization deep within the orthorhombic (o) phase above the triple point. Here we singled out crystals A–D. They start life as uniformly bright and regular, hence by our criterion in the h phase, just as in Figure 2, in which form they continue to grow (marked by arrows →). However, after a lapse of time at a certain stage of growth they transform, becoming blotchy, marked by arrow ⇒ (see, e.g., A in Figure 3c). This, by our assignment, means that the crystals, initially in the h form, have transformed into the o form.

Figure 4 represents the analogous situation below the triple point, but otherwise again in the o region. The appearance of the crystals here is, due to smaller number

of nuclei forming, particularly clear. The crystals appear again as uniformly bright lines, hence in the h phase, and continue to grow in this form (A–D in Figure 4a). A total of 8 min after the stage in Figure 4a, i.e., after 70 min of total crystallization time, crystal B becomes blotchy (Figure 4b), and so does, after 95 min, crystal A (Figure 4c), signaling transformation to the o structure, while C and D remain uniform, hence in the h form (arrows ➞ and ⟹ again have the same meaning as in Figure 3).

At this stage we may interpret our observations as follows:

(i) Crystallization always starts in the h form irrespective of whether in the h or o region of the phase diagram. Thus in the h region such crystals arise in their stable state and in the o region in a metastable state.

(ii) In the o region the initially metastable h form transforms into the stable o form after a certain lapse of time at a certain stage of growth, irrespective of whether above or below the triple point.

As a further step the melting behavior was examined through raising the temperature. Crystals grown in the h region (Figure 2) are seen to melt directly. This has been observed in earlier studies and, amongst others, used to determine the liquid-hexagonal crystal coexistence line in the phase diagram. This will not be illustrated separately as it is contained in the heating sequence of Figure 3 (crystal C in Figure 3e,f; see below).

Comparison between Figures 3 and 4 reveals the distinction in melting between a region above and below the triple point. Above the triple point we are passing from the o to the h region; hence, we expect the o crystals to transform to the h crystals correspondingly. Indeed, in Figure 3 we can see this transformation. E.g., crystals A and C (in Figure 3d), already in the o phase, change into the more uniformly bright line seen in frame 3e at a higher temperature situated in the h region. At the same time crystals still in the metastable h form while in the o region, e.g., D in frame 3e, stay uniformly bright, in fact grow further (the uniformly bright line increases in length) on passing into the h region. On raising the temperature further, beyond the melting temperature of the h phase, all crystals are seen to melt, apparent by gradual shrinkage of the bright lines (frame f). This includes crystals which first transformed from o to h structure (A–C) *and* crystals which have remained in the h phase still while in the o region (D).

The behavior of crystals arising in the region below the triple point is markedly different, as shown by the sequence Figure 4c–h. Here again we have the two kinds of crystal in the same field of view initially: the uniformly bright h crystals, which are the primary products of crystallization (C and D in frame 4e), and the o crystals of blotchy appearance (A and B in frame 4e) which, as we have seen previously from frames a–c, are transformation products of the initial h crystals. On heating, it is now the h crystals which melt first (C and D absent in frames e and f) while the rest remain unaltered. On further heating to still higher temperatures also the o crystals are seen to melt (A and B in frames f–h) followed here until their near disappearance in Figure 4h. Thus we see that in the region below the triple point the h crystals have the lower melting temperature, with both h and eventually o crystals melting without transformation, in contrast to crystals arising in the region above the triple point where the o crystals first transform into h crystals, the latter having the higher melting point. This well-defined, reproducible behavior, in particular the distinction of regions above and below Q, is consistent with the significance we have attached to

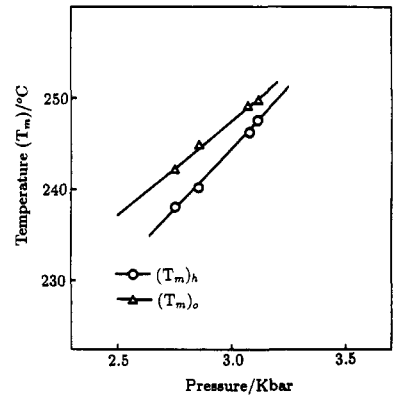

Figure 5. P–T diagram below the triple point; data collected optically during in situ melting. Temperature values shown are not absolute due to calibration uncertainties of the pressure cell.

the two optically distinct appearances of the crystals. This lends support to their respective assignment as metastable crystals in which form the crystals grow and stable crystals into which they transform subsequently with growth ceasing, yet the same transformed crystals melting at higher temperatures, providing self-contained optical evidence for the principal contentions of this paper.

When the by now well-tested optical distinction between h and o crystals was utilized, the melting temperatures of each at different pressures were determined below the triple point (Figure 5). The samples referred to by Figure 5 were all extended-chain crystals with thicknesses of either one or several chain lengths. The first to note is that there is a difference between the melting points of the h and o crystals, the latter melting at the higher temperature as to be expected from the foregoings, with the difference increasing continuously with decreasing pressure. The observation of melting temperatures was restricted by a lower limit of 2.5 kbar as crystals with extended chains could not be obtained below this pressure. (In light of the above it will be apparent that the usually applied DTA investigation of melting behavior on its own has its limitations and could give rise to misinterpretation. Because of the metastability of the h crystal, below the triple point, deduction of the two different melting temperatures for the h and o crystals might not have been possible by conventional DTA which has been used earlier for the mapping of P–T phase diagrams as in Figure 1. By this method alone, what might have been the melting of h crystals could have been interpreted as o → h transformation and the melting of stable o crystals by that of h crystals. This would have led to an assignment of the triple point below its true value.)

It will be immediately apparent that below the triple point there can be no o → h transformation; i.e., the o → h coexistence line is virtual, in contrast to P's above the triple point where such a transformation is real, where, however, the o–l coexistence line, i.e., T_m of the o phase, is virtual. All these considerations, coupled with the observation of two melting temperatures below the triple point, one for the h and another for the o phase, in fact the existence of an h phase within the o phase stability regime, require an extension of the phase diagram which we shall proceed to do in what follows.

3.2. Extension of the P–T Phase Diagram. A P–T phase diagram, which according to the foregoings is extended so as to include metastable regions and virtual phase transitions, is represented by Figure 6 in an idealized form. Here, to facilitate the presentation, the phase demarcation lines are drawn (i) as straight lines instead of curved as they generally are and (ii) as passing through

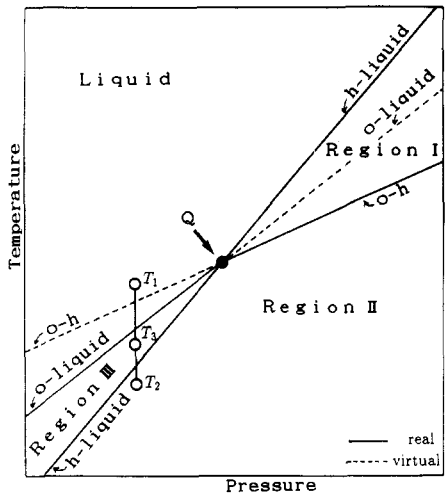

Figure 6. Schematic P–T phase diagram including metastable and virtual phase boundaries. T_1, T_2, and T_3 refer to the experiments under Figure 8.

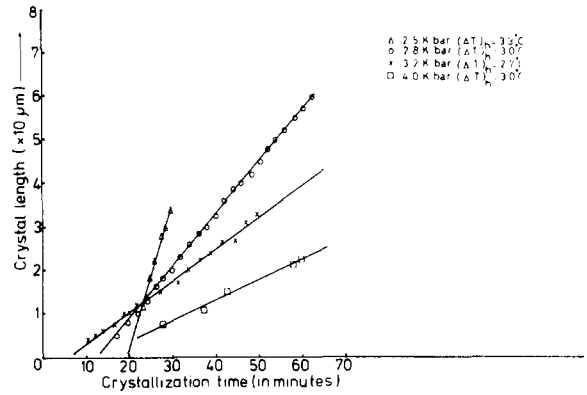

Figure 7. Lateral growth of h crystals showing linear increase with time, as obtained by the in situ optical studies (e.g., Figures 2–4) at preselected isobaric and isothermal conditions.

intersections (triple point) without change in direction, which is again an idealization. Here the heavy lines correspond to the state of ultimate stability for the appropriate P and T values, with all lines passing through a common point, which is the triple point Q. As stated earlier, we see in Figure 6 that above Q (in terms of P) we have the sequence orthorhombic (o)–hexagonal (h) → liquid, i.e., melt (l), with increasing T. Below Q we have o → l (i.e., melting of the o form) when the stable o phase only is considered and h → l (i.e., melting of the h phase) when melting of the metastable h phase is considered. As we have shown, h can exist as a metastable phase throughout the o stability regime studied here. In contrast, the o phase cannot be observed within the stability region of the h phase; hence, the o–l line, above Q (in terms of P), is unrealizable and so is the o–h line below Q. However, as will become apparent, irrespective of whether actually realizable or not, the extension of the phase demarcation lines into unstable regions has significance for the crystallization process.

The crystallization in stable h and o phases, along with the metastable h phase at the different temperatures and pressures, leads to the subdivision of the P–T phase diagram into three regions of significance for the present purpose. These regions are as follows:

Region I above the triple point (in terms of P) in between h–l and o–h transition lines corresponds to the stable h phase. Region II which extends over P's to below as well as to above the triple point, having the upper bound of h–l and o–h lines below and above the triple point, respectively, is the region of stability for the o phase, where nevertheless by present work the h phase can also exist as the metastable phase. Region III, which is in the stable o phase, is distinct by the fact that it cannot contain the h phase, even in the metastable form, because it lies above the h–l line. The significance of these zones will become apparent below. For what follows, Figure 6 is meant to stand for infinite extended-chain crystals; similar diagrams (appropriately displaced along the P and T axis) can be constructed for crystals smaller than infinite size including various folded configurations.

3.3. Lateral Growth Rates. Establishment of Linear Growth; Difference between h and o Crystals. The individual frames in each of the three micrographs in Figures 2–4 are arranged in order of increasing time and hence represent consecutive stages of crystallization within identical selected areas. Correspondingly, one can see crystals arise and grow. As most of the crystals are seen closely edge-on, where their visibility between crossed polars is maximum, their lateral growth is registered in the form of an increasing length of the bright lines, as is apparent from inspection of the series in Figures 2–4. This should enable the quantitative determination of lateral lamellar growth rates under constant pressure and temperature for selected P's and T's, as has been reported in the previous paper by one of us[12] (M.H.) which contains the relevant technical details.

Figure 7 is a selection of the measurements of lateral growth of preselected crystals under isobaric and isothermal conditions for P's above as well as below the triple point Q. The P and T (or rather ΔT) dependence will be commented on later. At this point we draw attention to the linear increase in crystal lengths within crystallization time, enabling characterization of the growth rates through the slope of each line for a given P and T to be enlarged upon further below. (Each line in Figure 7 refers to a specific selected crystal. At a given P and T there was some variation between different crystals while linearity pertained throughout. We attribute this variation to the fact (derived from electron microscopy) that some of the crystals could be elongated (leaf) shaped.[18,19] In such a case growth rate will be different in different directions which, as seen in random edge-on views, give rise to a spread in growth directions and rates as measured here. For representations like Figure 7 (and Figure 9) crystals with a maximum growth rate for each P and T were selected, which, as will be seen, give self-consistent results. In any event, variations between different crystals were small (typically at P = 4.0 kbar and $(\Delta T)_h$ = 2.5 °C, the two extreme lateral growth rates (V) were 0.1875 and 0.1428 μm/min) to override the conclusions. The origin of shape differences (leaf or circular) between crystals, to the best of our knowledge in the same h phase, is an issue of current topicality beyond the scope of this paper, to be discussed elsewhere.[19])

Linear increase of crystal size, and hence constant rate, is clearly as expected from the whole background of polymer crystal growth studies. While this is readily obtainable at atmospheric pressures, it is not so when enhanced pressure had to be applied by mechanical means. Namely, the volume of the material decreases during crystallization which, if P is to be maintained constant, the pressure-generating device has to follow. In contrast to pressure devices used in most preceding works in our type of cell construction, described in detail elsewhere,[12] the piston moves smoothly enough for it to follow volume changes during crystallization, which accordingly will occur strictly isobarically. This feature enables growth rates to

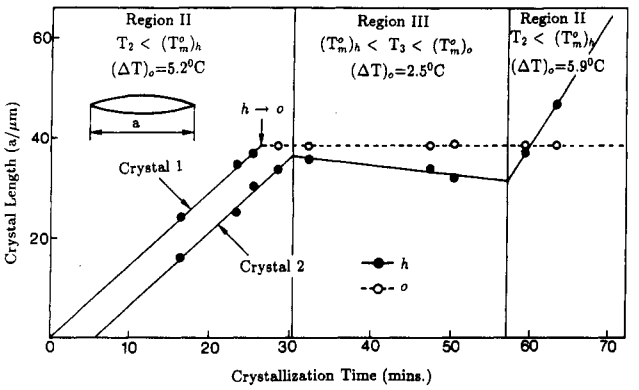

Figure 8. Examples of the effect of phase type on lateral growth of two crystals below the triple point. Both crystals 1 and 2 are in the h phase to begin with. Crystal 1 stops growing on its transformation into the o phase. Crystal 2 shows continuing growth and melting behavior in the h crystal form. *a* represents the crystal length as seen optically in Figures 2–4. T_1, T_2, and T_3 are the temperatures at isobaric condition as seen in Figure 6.

be determined isobarically and thus the investigations here described to be pursued. In what follows we shall first contrast the overall features of the lateral crystal growth in the different regions of the phase diagram, to be followed by a more quantitative examination of the supercooling dependence of the growth rates.

Distinction between the Behavior above and below *Q*; the Nongrowth Region Regime III. In region I the crystals were observed to grow at a constant rate, as long as they did not impinge on each other (when not unexpectedly growth stops). The crystals remain uniform in appearance throughout, which according to the foregoings signifies that they remain in the h phase untransformed as to be expected (Figure 2). In contrast, throughout region II, the crystals were seen to grow at a given constant rate, in fact to grow at all, only as long as they were in the h phase by our optical criterion. As described previously, these h crystals, metastable in region II, at some stage transform into the stable o phase. Here, invoking also the measurement of size increase, we now add that lateral growth is arrested when this transformation occurs: i.e., once in the o phase the crystals simply do not grow, at least on the time scale of our experiment. This can be readily seen from Figures 3 and 4 when comparing the untransformed and transformed crystals at consecutive times (➡ h and ⟹ o).

The above holds irrespective of whether we are above or below the triple point *Q*. In fact the *P* range in Figure 7 straddles the triple point. Nevertheless, in spite of the above-mentioned similarities, there are certain distinctive differences to which we shall turn in what follows.

Take first the situation below the triple point. The experiments to be reported here relate to the observations along an isobaric line such as defined schematically by T_1, T_2, and T_3, in Figure 6. This line is located at pressures below the triple point (*Q*), which means that nowhere along it can the hexagonal phase be the thermodynamically stable one. Figure 8 (see also ref 18) shows the development of two chosen crystals in a given field of view as a function of time after cooling from above the melt (point T_1), first to point T_2 (as represented schematically in Figure 6) and there held at constant temperature for 30 min. The crystals, by the optical criterion (Figures 2–4), are in the hexagonal form. As seen, they grow with identical constant rates. At some stage (26 min) crystal 1 is seen to transform into the orthorhombic form and concurrently it stops growing altogether (an effect repeatedly and reproducibly observed), while the still hexagonal crystal 2 continues to grow. At 30 min (in Figure 8) the temperature was raised to what corresponds to T_3 in Figure 6. The lateral size of crystal 1 in Figure 8 stays constant while that of crystal 2 diminishes, indicating that it is melting from the edge inward. When the temperature is lowered again to point T_2 (for schematics see Figure 6) at 56 min, no effect on the lateral orthorhombic crystal 1 could be observed but it reintroduces the growth of the still hexagonal crystal 2 at about the same rate it had during its first residence at that temperature (Figure 8). It needs adding that the crystals are all seen to grow with constant shape, the visually observed tapered or cigar-shaped contour being unaffected by the o → h transformation when this occurs (an issue to be commented on in subsequent work). We see that the content of Figure 8 expresses the significance of region III (within which point T_3 is situated): it will be apparent that region III, i.e., the region where the h phase cannot exist (without slowly melting; Figure 6), is also a "nongrowth" region.

Turning to the situation above the triple point, while still in region II, we find, as stated previously, that again all crystals start life in the h phase and transform to the o phase during growth. However, on raising the temperature isobarically, now we enter region I with consequent o → h transformation (the o → h demarcation line is here real) and, in contrast to the situation below *Q*, with continuing growth (Figure 3, for itemization see above).

***P* and *T* (or ΔT) Dependence of Growth Rates.** Being in a position to define lateral growth rates (*V*, the slopes of lines in Figure 7), we may explore their dependence on *P* and *T*. There are limitations on the conditions within which *V* could be examined: the crystals should not grow too rapidly to prevent growth to be followed nor too slowly for this to become impracticable, and further the crystals should not be too numerous nor too scarce. The *P* and *T* range to be presented here lies within these limits, encompassing the growth rate range of 0.1–40 μm min^{-1} as to be read off from Figure 9 (see below).

In what follows we shall express our temperatures in terms of supercooling ΔT as there is less error in the temperature difference than in the absolute temperature values due to positioning uncertainties of the thermocouple in our experimental arrangement. Here $\Delta T \equiv (T_m)_h - T_c$, where T_c is the chosen crystallization temperature and $(T_m)_h$ the temperature at which the crystal under observation melts when eventually heated above T_c. Of the two melting temperatures in Figure 5 (for a given *P*) here we take the lower one (marked by circles) which corresponds to the crystals while in the h phase (already implied by the subscript h in the notation for ΔT). The $(\Delta T)_h$ values thus determined have a reduced error limit within 0.5 °C (as compared to 2–3 °C for absolute values for *T*'s. We shall therefore proceed to express our results in terms of $(\Delta T)_h$ in what follows (as is indeed done already for Figure 7).

$(\Delta T)_h$ of course represents a supercooling in terms of which crystal growth rate data are usually analyzed. Here $(\Delta T)_h$, as opposed to $(\Delta T)_o$, is the natural choice, as it is in the h form that the crystals originate and grow; also as will be apparent, this leads to physically more satisfactory results. As the crystal thickness, while large by standards of usual chain-folded crystals, is still finite, $(T_m)_h$, as measured, may not be quite equal to the ultimate melting point of the fully extended chain crystal $((T_m°)_h)$; and this applies also to $(\Delta T)_h$. To ensure that variations in $(T_m)_h$, and hence in $(\Delta T)_h$, due to this source are minimized and that we are as close to $(T_m°)_h$, and hence to the $(\Delta T)_h$

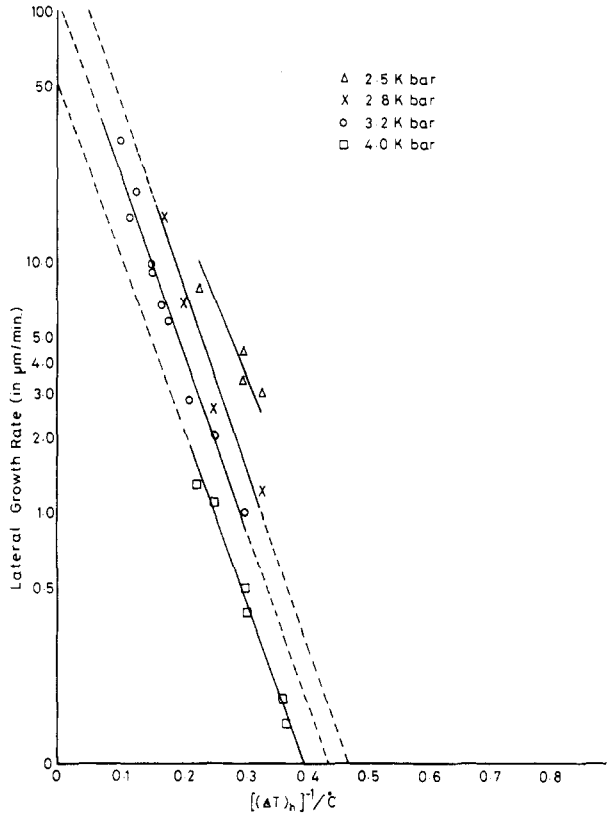

Figure 9. Lateral growth rate of h crystals as a function of inverse supercooling at different pressures. Supercooling is with respect to the melting of the h phase.

defined for the infinite crystal, as possible, the following procedure was adopted: After completion of measurement in linear growth rate at a chosen T_c, the temperature was raised so as to locate the temperature at which the crystal, still within the h phase, melted. Then the temperature was lowered to the highest T_c where crystals were still appearing and growing with still the identical sample in position. It was the melting point of these latter crystals, which thus attained the highest achievable thickness for the given P in question, which was used for defining $(\Delta T)_h$ at that pressure. We then found that, when expressing V in terms of $(\Delta T)_h$, thus determined by direct measurement, displayed sufficient resemblance to the behavior pattern expected from the customary dependence on the true supercooling (i.e., with regards to $T_m°$) to justify the present pragmatic approach as a first step in analyzing the results.

In Figure 9 we plot V as a function of $(\Delta T)_h^{-1}$ for a range of P values. Here V is taken from slopes of crystal size vs time lines such as in Figure 7 (and further ones not shown separately). We see that to a first approximation these fall on a straight line with a negative slope thus consistent with a relation such as

$$V = A \exp[-B/(\Delta T)_h] \quad (1)$$

Equation 1 of course has the form appropriate to secondary nucleation-controlled crystal growth adopted throughout past works on polymer crystallization.

In Figure 9 the different lines span different ΔT ranges (the lack of full overlap is due to the practical limitations of following crystal sizes accurately as a function of time, at *all* the relevant P and T values as pointed out above). Even so, there is good overlap between lines for P's of 3.2 and 2.8 kbar: as seen they can be considered as closely parallel. The same applies to the lines for 4.0 kbar, however, here with an appropriate vertical shift. Data points for the lowest P, 2.5 kbar, span the narrowest ΔT range and cluster at the highest V values, making the slope assignment less certain; even so, the slope cannot be significantly different from the rest even if by data available it could be somewhat lower.

All in all, the functional relation in eq 1 seems closely obeyed with a common slope, hence B. The best fit to our experiment yields B = 15.4 K.

Further, even with the above qualifications (i.e., only partial or no overlap in terms of ΔT and P range), it is apparent that there is a systematic shift of the lines in Figure 9 with P in a sense that, for a given $(\Delta T)_h$, V is greater for lower P. In terms of eq 1 this means that A is a decreasing function of P. Numerically our A values are 49.8 μm/min at 4.0 kbar, 110.6 μm/min at 3.2 kbar, and 229.8 μm/min at 2.8 kbar. Amongst these the values for P = 3.2 and 2.8 kbar are the most reliably defined: even within this small P range the shift to higher A's with decreasing P is apparent.

There remains the significance of the constants. The constant B is an activation barrier to growth, whether nucleation determined[1] or entropic.[2] Our results signify that this is largely pressure insensitive, at least within the P range examined. The constant A contains the effect of chain transport within the melt, a frequency, and a survival factor. Our results thus mean that the above factors respond significantly to application of pressure in a sense of increasing pressure hindering crystal growth. That pressure should hinder transport in particular, where the latter is related to chain mobility, seems very reasonable.

Next we may scrutinize the choice of $(T_m)_h$, and the corresponding $(\Delta T)_h$, out of the two melting temperatures featured in Figure 5. We did perform the plotting as in Figure 9 for $(\Delta T)_o$, in place of $(\Delta T)_h$, except for P's above Q where $(T_m)_o$ is not known from direct measurement (not to be illustrated). As to be expected, the straight line relation itself is retained on changing reference for ΔT. However, the pressure dependence becomes inverted, i.e., for the same $(\Delta T)_o$ value V was higher for larger P, a result contrary to the simple argumentation applied for Figure 9. This provides added support to the self-evident choice for taking the T_m value which pertains to the form in which the crystals are seen to grow (i.e., the h form). (Incidentally, without the present experimentation this important point, namely, that it is the $(T_m)_h$ which really matters, would have remained overlooked by potential future works in this field, as it may have done in the past already.)

At this stage we may profitably compare the new results with those obtained by one of us previously.[12] These earlier works using the present apparatus design were carried out for one selected pressure, 3.0 kbar (chosen to lie just below Q). It has led to the establishment of constant growth rates at that pressure with B = 12.6 K and A = 204 μm/min. Our new results agree remarkably well with the above: B is within 25% and A, when interpolating to 3.2 kbar, is nearly identical. In general, this gives us confidence in the reproducibility of the technique and in the consistency of the phenomena under study and, more specifically, in the extension of the investigation over a range of pressures, which was the main objective of the present work. It is most notable, in particular, that in ref 12 $(T_m)_h$ was taken as reference for the undercooling, as a direct result of measurement, before the full implications, as revealed by the present work, have become apparent. The agreement over the P and ΔT regions, in the case where the two successive works overlap, now gives a posterior justification to the previously adapted procedures and choices.

4. Summary of Experimental Results

The above results can be summed up as follows.

(i) The mobile hexagonal form of polyethylene can exist as a metastable phase in the stability region of the orthorhombic form and in fact plays a decisive role in the primary crystallization process. This applies both above and below the triple point.

(ii) Below the triple point, crystals in the h and o phases melt individually without going through any transition; the melting temperature of metastable h crystals is lower than that of the stable o crystals. From this the existence of a nongrowth region in the P–T phase diagram follows.

(iii) Above, as well as below, the triple point within our P and ΔT range explored so far, crystals can only grow in the h phase, in spite of the fact that below the triple point the thermodynamic driving force (supercooling) is greater in the o phase. This is supported not only by the verification of such growth in itself but also, most strikingly, by its stoppage on h → o transformation.

(iv) Both above and below the triple point in the P–T phase diagram it is the supercooling corresponding to the h crystals which controls the lateral growth rate of crystals, instead of the larger supercooling from the melting temperature of the o crystals, which correspond to the state of thermodynamic equilibrium.

(v) The activation for growth is found to be unaffected by P, but that of the transport (and survival) term is pressure sensitive, resulting in a decrease in growth rate with increasing P for constant supercooling with respect to the h phase $(\Delta T)_h$ and, conversely, to an increase in growth rate with decreasing P.

5. Implications for Polymer Crystallization

The foregoing in general, and the last point in particular, invites the question as to how far the new points raised by this work are pertinent to polymer crystallization as usually observed. Previous high-pressure work relied on the phase diagram and consequent delineation of phases: accordingly, in the context of polyethylene, all that was different from common experience was thought to be identified by happenings in region I and the newly recognized hexagonal phase therein. However, the present work shows that this hexagonal phase can exist also as a metastable, transient, highly mobile mesophase, also in the stability region of the usual orthorhombic crystal form with decisive influence on the crystallization behavior. In light of this, two possibilities arise.

First, the newly found behavior that formation and growth of crystals requires the presence of the mobile phase under all circumstances. Second, there is a changeover in the mode of crystallization to that involving the orthorhombic phase alone when approaching the more familiar conditions under atmospheric pressure.

It will be apparent that the issue is fundamental with important implications in either case. The factor common to both is that the phase diagram, and hence thermodynamics, ceases to give a unique guidance. Regarding the first alternative, an extension of Figure 5 down to atmospheric pressures is invited to see whether the nongrowth region III could account for the large supercooling normally required for crystallizing polyethylene (i.e., practicable growth rate only at $T_c \leq 130$ °C and below, when $(T_m°)_o$ is 145 °C). This is clearly a novel and exciting possibility. Alternatively, if the mode of crystallization changed (second possibility), then it would be essential to find the P and T where this takes place (see also ref 19).

Whatever the answer to the above open questions it is clear that the above definitive effects, and inferences drawn therefrom, should have implications for our existing conceptions of crystal growth.

We conclude by drawing attention to the fact that the present type of experimentation can provide information on actual processes occurring at the inception of crystal growth, such as were unobtainable before, correspondingly furthering our insight into polymer crystal growth.

Acknowledgment. Our thanks are due to Dr. Hoffman for providing us with the invaluable PE fractions. Financial support by SERC making this work possible is gratefully acknowledged.

References and Notes

(1) Hoffman, J. D.; Frolen, L. J.; Ross, G. S.; Lauritzen, J. I., Jr. *J. Res. Natl. Bur. Stand. (U.S.)* **1975**, *79A*, 671.
(2) Sadler, D. M. *Nature* **1987**, *326*, 174. Sadler, D. M.; Gilmer, G. H. *Polymer* **1987**, *28*, 242.
(3) Hikosaka, M. *Polymer* **1987**, *28*, 1257; **1990**, *31*, 458.
(4) Wunderlich, B.; Melillo, L. *Makromol. Chem.* **1968**, *118*, 250.
(5) Bassett, D. C.; Khalifa, B. A. *Polymer* **1973**, *14*, 390; **1976**, *17*, 275.
(6) Bassett, D. C.; Khalifa, B. A.; Turner, B. *Nature* **1972**, *239*, 106; **1972**, *240*, 146.
(7) Ungar, G. *Macromolecules* **1986**, *19*, 1317.
(8) Wunderlich, B. *J. Polym. Sci. B* **1967**, *5*, 7.
(9) Calvert, P. D.; Uhlmann, D. R. *J. Polym. Sci., Polym. Phys. Ed.* **1972**, *10*, 1811. Yasuniwa, M.; Enoshita, R.; Takemura, T. *Jpn. J. Appl. Phys.* **1976**, *15*, 1421.
(10) Bassett, D. C.; Block, S.; Piermarini, G. *J. Appl. Phys.* **1974**, *45*, 4146.
(11) Bassett, D. C. *Polymer* **1976**, *17*, 460.
(12) Hikosaka, M.; Seto, T. *Jpn. J. Appl. Phys.* **1982**, *21*, L332.
(13) Hikosaka, M.; Seto, T. *Jpn. J. Appl. Phys.* **1984**, *23*, 956.
(14) Hikosaka, M.; Tamaki, S. *J. Phys. Soc. Jpn.* **1981**, *50*, 638.
(15) Hikosaka, M.; Tsukijima, K.; Rastogi, S.; Keller, A., submitted for publication in *Polymer*.
(16) Hikosaka, M.; Kawabata, H.; Keller, A.; Rastogi, S. *J. Macromol. Sci. B*, in press.
(17) Bassett, D. C. *Developments in Crystalline Polymers—1*; Bassett, D. C., Ed.; Applied Science Publishers: London, 1982; p 115.
(18) Hikosaka, M.; Seto, T.; Kawabata, H.; Keller, A. *Polym. Prepr. Jpn.* **1988**, *37*, 2519.
(19) Rastogi, S.; Hikosaka, M.; Kawabata, H.; Keller, A. *Makromol. Chem., Macromol. Symp.*, in press.

Registry No. PE (homopolymer), 9002-88-4.